CHAPTER I

Introduction

1.1 Evolution of nanotechnology

Technological revolution always comes along with political and social changes. When the advancement in the technological change is huge, social changes also occur to adapt to accommodate this objective reality [1]. For example, as farmers started to gather wealth (that is, food) for communities, an army became necessary to protect it. Soon after World War II, governments worldwide and specially in the US realized that considerable investment in the natural sciences could radically affect the power and wealth of nations. Integrated electronics, internet and even lasers can be summarized into the age of information and telecommunications as a direct result of this investment. A huge part of nanotechnology naturally follows from these lines of technical chase and scientific inquest [1]. Along with the theoretical understanding of quantum physics and electrodynamics that has advanced over the last century, this prolonged research has led us to incredible rewards from the manipulation and control of matter at the nanoscale. Consequently there has been a surge in the research of science of nanomaterials.

1.2 Nanoscale Materials

Nanoscale materials are defined as a set of substances with at least one dimension less than approximately 100 nanometers. A nanometer is one millionth of a millimeter - approximately 100,000 times smaller than the diameter of a human hair [2]. Nanomaterials are of prime interest because due to small size, unique optical, magnetic, electrical, and other properties emerge. These developing properties have the prospective for great impacts in electronics, medicine, and other fields. Some nanomaterials occur naturally, but of particular interest are engineered nanomaterials (EN), which are designed for, and already being used in many commercial products and processes [2]. They can be found in such things as sunscreens, cosmetics, sporting goods, stain-resistant clothing, tires, electronics, as well as many other everyday items, and are used in medicine for purposes of diagnosis, imaging and drug delivery [2].

1.2.1 Different kinds of nanomaterials

The nanoscale materials are basically divided into two types namely metallic [3] and semiconductor [4] nanoparticles. Semiconductor nanoparticles possess distance in eV

between valence band and conduction band energy levels and this difference in energy levels of conduction band minima and valence band maxima defines the band gap of the particle. This Band gap is generally larger than the bulk counterpart.

However, no band gap is observed in case of metals, so tuning the band gap with size is not feasible; but the band dispersions reveal that the curvature of the bands at the edges is high compared to curvature at the centre of the band in the case [5].

Unlike the bulk state which is characterized by semi continuous energy spectrum, nanoscale materials possess discrete energy levels.

1.2.2 Properties of nanomaterials

1.2.2.1 *High surface to volume ratio*

The surface of a sphere scales with the square of its radius *r* whilst its volume scales with r^3. The total number of atoms *N* in this sphere is linearly proportional to volume. The fraction of atoms at the surface is called dispersion *F*, and it scales with surface area divided by volume, i.e. with the inverse radius or diameter, and thus also with $N^{1/3}$ [6]. The same relation goes for long cylinders of radius *r* as well as for thin plates of thickness *d*. atoms at surfaces have fewer neighbours than atoms in the bulk. Owing to this lower coordination and unsatisfied bonds, surface atoms are less stabilized than bulk atoms. The smaller a particle the larger the fraction of atoms at the surface, and the higher the average binding energy per atom. Since the surface-to-volume ratio scales with the inverse size, there are numerous properties which obey the same scaling law including melting point and other phase transition temperatures [6]. Also since most of the atoms lie on the surface, the reactivity is greatly enhanced in case of nanoparticles. The presence of maximum percentage of total atom on the surface causes various surface defects with states related to definite energy state referred as surface states which are liable for overall changes in other energies corresponding new energy states [7]. These surface states also play a vital role as electron trap centres as they participate in different electronic transitions [8]. Their influence can be observed in luminescence, photocatalytic activity and single electron tunneling phenomena [9].

1.2.2.2 *Quantum Confinement effect*

This is a typical size effect found in semiconductor nanocrystals [10]. As the material goes from bulk to nano phase, its optical as well as electronic properties vary [11]. The scale of the transition is determined by a parameter which is known as Bohr exciton radius, an intrinsic property of the material [12]. In a direct band gap semiconductor the valence and conduction bands possess same K vector and upon absorption of photons of appropriate wavelength bound electron hole pair known as *excitons* are created. When the size of the semiconductor comes to a comparable range with excitonic Bohr radius, the electronic properties start to change from the corresponding bulk state [13]. The confinement can be divided into three regimes according to the relationship between the microcrystalline radius R and R_B the bohr excitonic radius of its bulk counterpart where , $2R_B = a_e + a_h$, If $R>>R_B$, (a_e is the radius of electron and a_h is the same for hole) then that regime is called weak confinement. When $R<<a_h$ and $R<<a_e$, then it is called strong confinement regime. Another type of confinement regime is observed in very small micro crystallites where $R<< a_e$ but $R>>a_h$. This regime is known as medium confinement regime [14]

1.2.2.3 *Enhancement of band gap and blue shift*

In metals and semiconductors, the electronic wave functions of conduction band electrons are delocalized over the entire particle. Electrons can therefore be described as ‘particles in a box’, and the densities of state and the energies of the particles depend significantly on the size of the box, which at first leads to a smooth size-dependence [6]. However upon addition of more atoms, the shells get filled up and discontinuities crop up when a new shell at higher energy starts to be occupied. Owing to these discontinuities, there is no easy scaling. Instead, one finds characteristics similar to that of atoms, with filled shells of extra stability. Such clusters are often named as ‘pseudo-atoms’. The band gap of semiconductor nanoparticles and therefore their absorption and fluorescence wavelengths become size dependent [6]. Ionisation potentials and electron affinities are tuned between the atomic values and the work function of the bulk material by changing the cluster size. These same properties relate to the accessibility of electrons for forming bonds or getting involved in redox

reactions. Thus the catalytic activity and selectivity become functions of size of the nanocrystal [6].

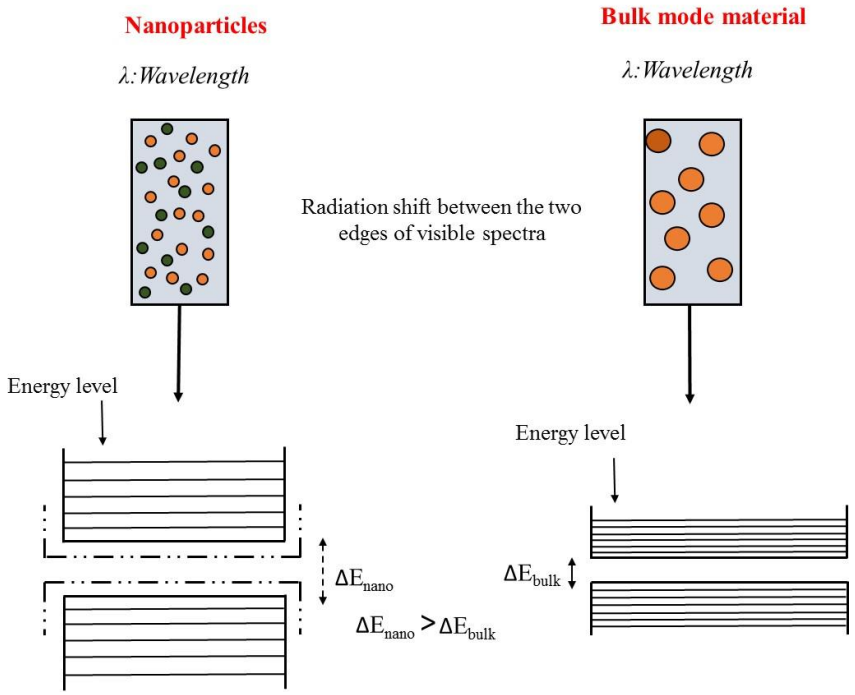

Fig 1.1: Change in band gap when the particle size is reduced from bulk to nano

The effect of enhanced band gap is accompanied with blueshift (towards lower wavelength) in the absorption spectra [15]. The effective mass approximation model is a theoretical model to understand the increasing band gap as well as blue shift.

1.2.3 *TYPES of nanostructures and density of states*

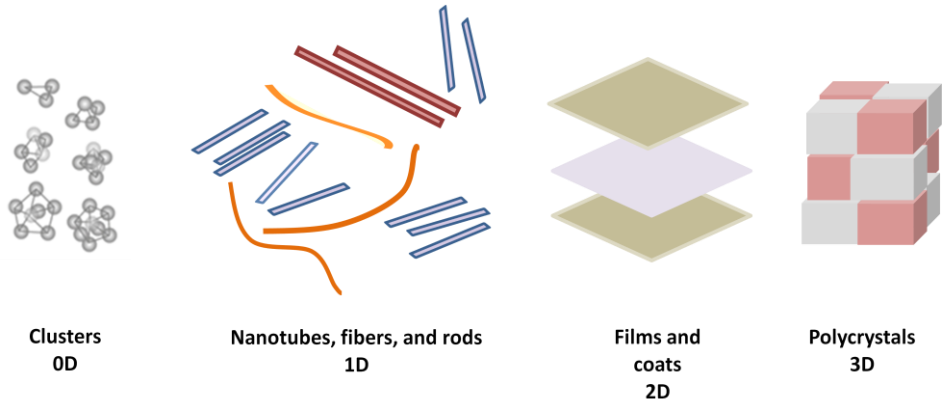

Fig 1.2: Different types of nanomaterials [16]

Nanomaterials can be divided into the following classes according to the size confinement effects:

Zero dimensional (0D): Materials wherein all the dimensions are measured within the nanoscale (no dimensions, or 0-D, are larger than 100 nm).The most common representation of zero-dimensional nanomaterials are nanoparticles. Nanoparticles can be amorphous or crystalline. They can exhibit various shapes and forms also can exist individually or incorporated in a matrix. They can be metallic, ceramic, or polymeric. Quantum dots (QD) are 0D nanocrystals [16].

One dimensional (1D): In this type of nanomaterial, the movement of the electrons are restricted in two dimensions and allowed in one dimension. The examples are nanorod, nanotube, nanowire etc.

Two dimensional (2D): In this type, the movement of the electrons are restricted in one dimension whilst movement is free in two dimension [17]. In such system, at least one of its three dimensions ranges in the order of the size of Bohr excitonic radius. Examples of this type are: nanofilms, nanolayers and nanocoatings.

Three dimensional (3D): They are generally bulk materials that are not confined to the nanoscale in any dimension. These materials are thus characterized by having three arbitrarily dimensions above 100 nm. Materials possess a nanocrystalline structure or involve the presence of features at the nanoscale. In terms of nanocrystalline structure, bulk nanomaterials can be composed of a multiple arrangement of nanosize crystals, most typically in different orientations.

The DOS (density of state) for the above types are mentioned below

For 0D (QDs), DOS has the shape of δ peaks

$$\frac{dN}{dE} \propto \frac{d}{dE} \sum_{\epsilon_i < E} \theta\,(E - \epsilon_i) = \sum_{\epsilon_i} \delta\,(E - \epsilon_i)$$

For 1 D (quantum wire)

$$\frac{dN}{dE} \propto \frac{d}{dE} \sum_{\epsilon_i < E} (E - \epsilon_i)^{1/2} = \sum_{\epsilon_i < E} (E - \epsilon_i)^{-1/2}$$

For 2 D (quantum well)

$$\frac{dN}{dE} \propto \frac{d}{dE_{\epsilon_i<E}} \sum (E - \epsilon_i) = \sum_{\epsilon_i<E} l$$

For 3D (bulk semiconductor)

$$\frac{dN}{dE} \propto \frac{dE^{\frac{3}{2}}}{dE} = E^{1/2}$$

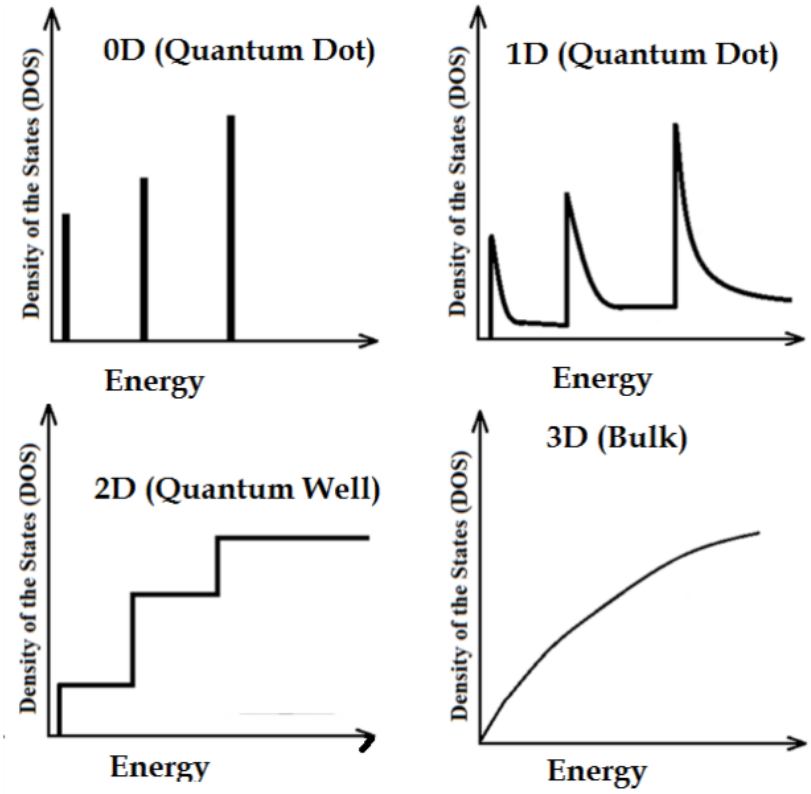

Fig 1.3: Variation of density of states vs energy

Where ϵ_i are discrete energy levels, θ is the Heaviside step function and δ is the Dirac function [19]. The variation of density of states (from continuous to discrete) with reducing dimensions is shown in fig 1.3.

1.2.4Core-shell Nanostructures

The broad area of nanoparticles can be categorized into simple and core-shell or composite nanoparticles based on single or multiple materials. As the name suggests, simple nanoparticles are made from a single material; whilst composite and core-shell

particles are composed of two or more materials. The core-shell type nanoparticles comprise of a core (inner material) and a shell (outer layer material) [20]. The choice of shell material of the core-shell nanoparticle is usually sturdily dependent on the end application and use. These type of nanoparticles are gradually grabbing more and more attention, since these nanoparticles have emerged at the frontier between materials chemistry and many other fields, such as electronics, biomedical, pharmaceutical, optics, and catalysis. They are highly functional materials with modified properties [20]. At times properties arising from either core or shell materials can be completely different. The properties can be tuned by changing either the constituting materials or the core to shell ratio [21]. Due to coating of the shell material, the properties of the core particle such as reactivity decrease or thermal stability can be modified, so that there is an increase in the overall particle stability and dispersibility of the core particle. Eventually, particles exhibit distinctive properties of the different materials employed together. This is especially true of the inherent ability to maneuver the surface functions to meet the miscellaneous application requirements [22,23]. Current applications of various core-shell nanoparticles are summarized by Karele and his co workers [24]. The individual reports from different researchers also throws light to the fact that core-shell nanoparticles are vividly used in different applications such as biomedical [25,26] and pharmaceutical applications [23] catalysis [22,27] electronics [28,29] enhancing photoluminescence [30,31] creating photonic crystals [32] etc. Particularly in the biomedical field, most of these particles are applied for bioimaging [33-35] controlled drug release [35-36], targeted drug delivery [33,35,37,38] cell labeling [33,39,40] and tissue engineering applications [36,41]

Based on their material properties, the core/shell nanoparticles can be divided into four main groups: (i) inorganic/inorganic; (ii) inorganic/organic; (iii) organic/inorganic; (iv) organic/organic.

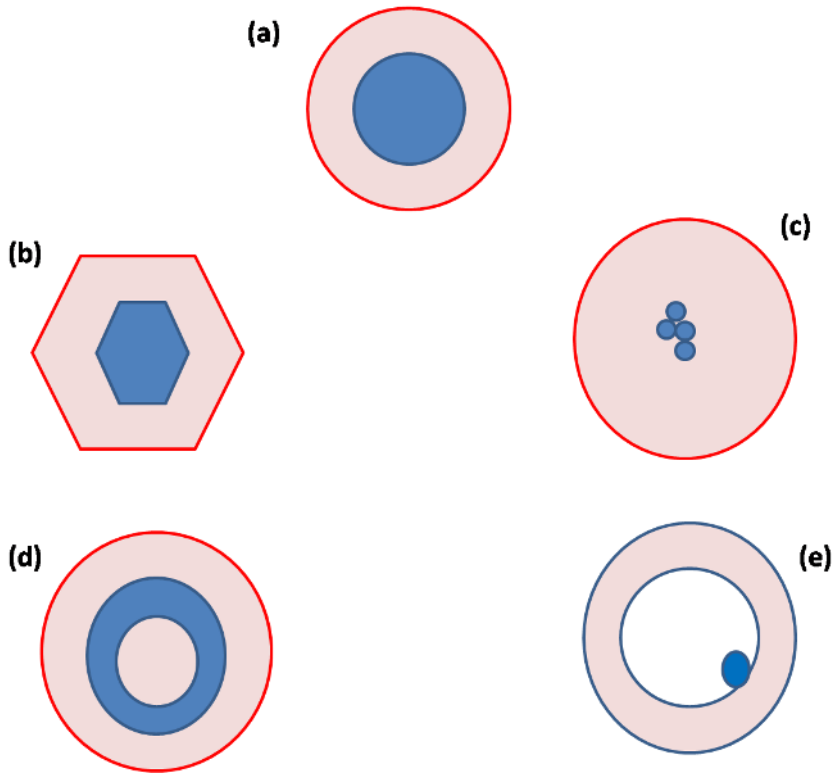

Fig. 1.4 Core-shells of various shapes [19]

One part of the inorganic/inorganic core-shell is semiconductor core-shell which we are going to deal in the next chapters. Semiconductor core-shells are also divided into two sub parts:

Semiconductor/non-semiconductor core/shell: In this type, either the core or shell is prepared of a semiconductor material with the remaining layer either metal, metal oxide, silica, or any other inorganic material [42-43]. This variety of core/shell nanoparticles has also found important place among the different inorganic/inorganic core/shell nanoparticles because of their aptness for more advanced applications in a wide range of fields extending from electronics to biomedical.

Semiconductor/semiconductor core/shell: In the recent decades, instead of using either a single semiconductor material or semiconductor/non-semiconductor core-shell material, researchers have emphasized on semiconductor/semiconductor core-shell materials to enhance the efficiency and decrease the response time. A particular interest is bestowed upon particles where both the core and shell are comprised of a semiconductor material or a semiconductor alloy [28,30,44,45,46]. They are again

classified in three parts:

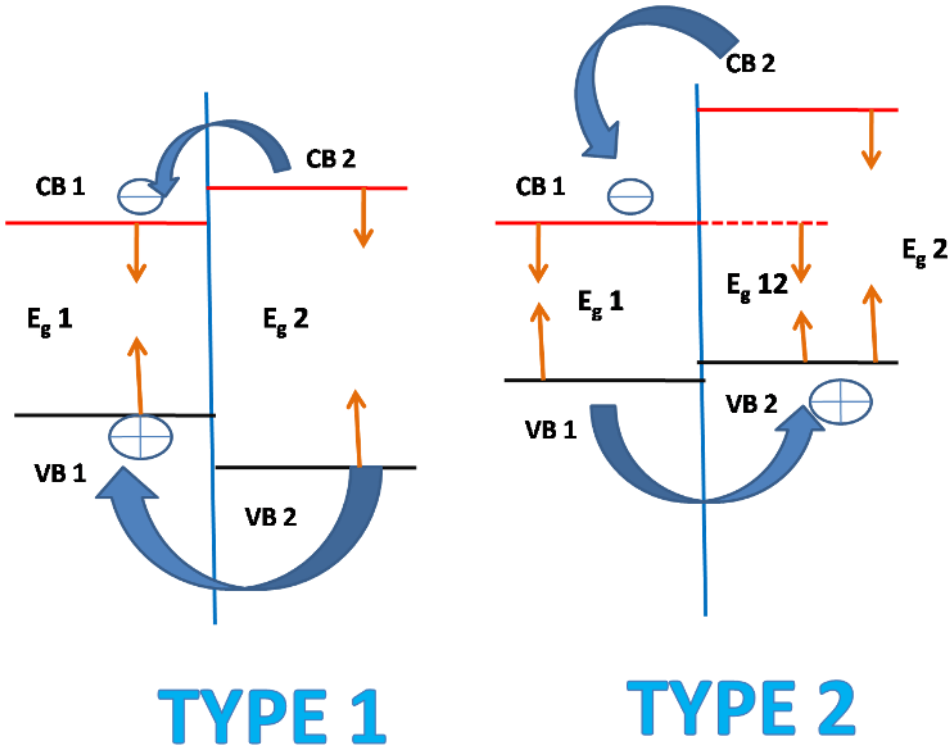

Fig 1.5: Band alignments in TYPE 1 and TYPE 2 core-shell structures [19]

TYPE 1: In this category, the energy band gap of the shell material is wider than the band gap of the core material. The electrons and holes are trapped within the core material because both the conduction and the valence band edges of the core are located within the energy gap of the shell [47]. As a result, the emission energy is estimated by the energy gap of the core material (Eg1). Fig 1.5 (left) schematically shows this type 1structure, where the conduction band of the shell is of higher energy (the higher band gap material) than that of the core. The valence band of the shell is also located at a lower energy than that of core. This arrangement of energy levels is important in order to confine the charge carriers within the core material. The shell is used to passivate the surface of the core with an aim to enhance its overall optical properties. Another role of the shell is to distinguish the more optically active core surface from its surrounding environment.

REVERSE TYPE 1: This group is the inverse of the one discussed above. In this class, the narrower band gap shell material is coated over the wider band gap core

material. Here, both hole and electron charges are partially delocalized on the shell materials and emission wavelengths can be modified by varying the thickness of the shell. Within this category, the most extensively reported systems are CdS/CdSe [48,49] and ZnS/CdSe [28]. They possess low quantum yields and higher resistance against photobleaching, whereas the quantum yield can be improved by coating another semiconductor material of a wider band gap.

TYPE 2: The third group of this category is known as type 2. In contrast to type 1, here, both the valence and conduction bands of the core are aligned at either lower or higher than those in the shell. As a result, one carrier is mostly confined to the core, while the other trapped the shell. Therefore, the energy gradient prevailing at the interfaces tends to spatially separate the electrons and holes on different sides of the heterojunction [47, 50]. This type of nanocrystals are more suitable for photovoltaic or photoconduction applications because of the separation of charges in the lowest excited states. The energy gap in this type of material (E_g12) is determined by the energy separation between the conduction band edge of one semiconductor and the valence band edge of the other semiconductor. Eg12 can be related to the conduction (U_c) and valence (U_v) band energy offsets at the interface by the following equation:

$$E_g 12 = E_g 1 - U_v = E_g 2 - U_c$$

Where E_g1and E_g2 are the band gaps of semiconductors 1 and 2, respectively. In this case, emission is lower than the band gap of either semiconductor. Some common examples of these types of particles are CdTe/CdSe [50-51] CdTe/CdS [52] ZnTe/CdS [53] PbTe/CdTe [45] ZnTe/ZnSe [54] CdSe/ZnSe [50] PbSe/CdSe [55] ZnSe/CdSe [56] and CdS/ZnSe [47].

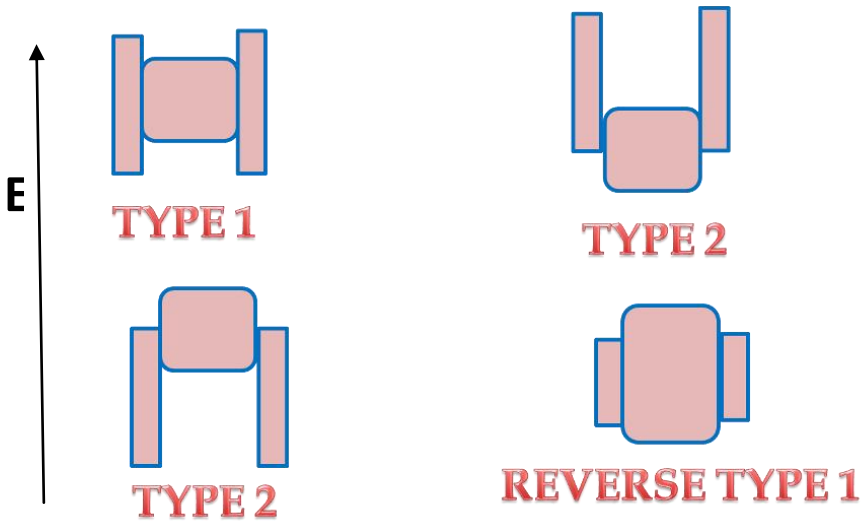

Fig. 1.6 Band alignments in different types of core-shell structure [19]

Approaches for core-shell nanostructures

Approaches for nanomaterial synthesis can be widely categorized into two parts: "top-down" and "bottom-up". The "topdown" method generally deals in traditional workshop or microfabrication methods where externally controlled tools are used to cut, mill, and shape materials into the desired shape and order. For example, the most common techniques are lithographic techniques (e.g., UV, electron or ion beam, scanning probe, optical near field) [57-58] laser-beam processing [59] and mechanical techniques (e.g., machining, grinding, and polishing) [60-61]. On the other hand, "Bottom-up" approaches utilize the chemical properties of the molecules causing them to self-assemble into some useful conformation. As far as the synthesis of core-shell nanoparticles is concerned, since ultimate control is necessary for achieving a uniform coating of the shell materials during the particle formation, the bottom-up approach has been established as more suitable. A combination of these two approaches can also be employed, such as after synthesizing the core particles by the top-down approach but then coating by a bottom-up approach in order to maintain uniform and precise shell thickness. To have a precise control over the size and shell thickness, instead of a bulk medium, using a microemulsion is preferable because water droplets act as a template or nanoreactor.

Synthesis of core-shell nanostructures

Generally, core-shell nanoparticles are synthesized with a two-step process, first synthesis of core and second the synthesis of the shell. The synthesis techniques of core-shell nanoparticles can be classified into two catagories depending on the availability of core particles: (i) the core particles are synthesized and separately incorporated into the system with proper surface modification for coating the shell material [62-64] (ii) the core particles are synthesized in situ, and this is followed by coating of the shell material [65-66]. Amongst the various methods for synthesis of core-shell particles used by different research groups are precipitation [67-68] polymerization [69-70] microemulsion, solgel condensation [20] layer by layer adsorption techniques [71-72] etc. But even after all sincere efforts to control the thickness and uniform coating of the shell using these methods, the methods are still not well established, and proper control is found as very difficult. The main hurdles are (i) agglomeration of core particles in the reaction media, (ii) preferential formation of separate particles of shell material rather than coating the core, (iii) incomplete coverage of the core surface, and (iv) control of the reaction rate. Generally for modification of core surface, surface active agents [73] and polymers [73-74] are often used by different research groups.

Review of works on core-shell nanostructure

Recently, there has been an increasing demand to obtain appropriate alternative energy sources. It has been established that quantum dot solar cells are good candidates for potentially low cost photovoltaic (PV) devices to use solar radiation as renewable energy [75] Regarding TiO_2, having a wide band gap (3.2 eV) in the UV region absorbs only 5% of the solar spectrum, resulting in poor conversion efficiency in solar cells applications. That is why, recent research has been emphasized on lowering the band gap of the TiO_2 to the visible region. Semiconductors which absorb in the visible regime such as CdS [76] PbS [77-78] Bi_2S [76-77] CdSe [79] and InP [80], can act as sensitizers as they are able to transfer electrons to large band gap semiconductors such as TiO_2 or SnO_2. K. Das and co-workers fabricated TiO_2@CdS type-II core-shell nanorods by a simple surface-functionalized method. The photocurrent density of the core-shell nanorods was found to be 212 times greater than that of the bare TiO_2

nanorods for a bias voltage of 5 V. The spatial separation of the charges, spatially indirect transitions, and surface passivation by shell played a vital role in increasing lifetime and photo current density.

Nanoscale building blocks comprised of II-VI compounds are of particular interest, as their synthesis and properties have been thoroughly studied experimentally over the past two decades [81-84, 50]. Interfaces are extremely significant morphological features that are key to determining the function of multi component nanostructures for light-harvesting applications. The electronic structure of nanoscale interfaces is expected to vary distinctly from bulk due to confinement, non-bulk-like electrical and mechanical boundary conditions, and surface reconstruction and passivation effects. Owing to quantum confinement, the band gaps and offsets are size dependent: band gaps increase with decreasing size, and incomplete screening associated with a confined interface can alter the interface dipole and band offsets. Additionally nanoscale heterojunctions can potentially endure larger lattice-mismatch than planar heterojunctions [84-85] and the resulting strain or presence of defects at nanoscale interfaces could further shift energy levels and band offsets as in strained bulk heterojunctions [86]. Also surface reconstruction and ligand passivation are expected to have a significant impact on the electrical and optical properties of the nanocrystals [87].Mostly explored core-shell structures of type-II catagory NCs include such combinations of materials as CdTe/CdSe [50] CdTe/CdS [88] CdTe/CdSe [89] ZnTe/CdS [90] and ZnTe/CdTe [90]. S. Evanov and co-workers studied the use of CdS and ZnSe, which are more stable in the colloidal form than Te-based semiconductors, for fabricating heterostructures that can exhibit the type-II localization regime [47 ,56, 91]. They applied an “inverted” core/shell design, in which a core of a wide-gap ZnSe was overcoated with a narrower-gap CdSe. These NCs exhibited high emission QYs up to 80-90%. 15 An interesting property of these structures was observed as they are tunable between type-I and type-II regimes that can be achieved by simply varying the shell thickness for a fixed core radius [91]

In photoexcited QDs, the main hurdle arises due to exciton-exciton annihilation process that occurs on the 10 to 100 ps time scale. So it becomes essential to dissociate the exciton by ultrafast charge transfer to electron donors and acceptors before the annihilation process [92]. There are few reports accessible in the literature on ultrafast

exciton (bound electron-hole pair) dissociation in QDs by electron transfer (ET) or by hole transfer to adsorbed acceptors, however, mechanism and rate of charge transfer are still to be studied effectively [93-94]. Considerable research efforts have been dedicated to charge transfer dynamics of type II semiconductor QDs. [95-97]. Bawendi and co-workers 10c reported the time-resolved emission in CdSe/ ZnTe and CdTe/CdSe where they have shown that charge recombination time in CdSe/ZnTe can be increased from 9.6 to 57 ns. It has also been investigated on ultrafast charge transfer dynamics of CdTe/CdS core-shell using femtosecond time-resolved absorption spectroscopy. Chen and co-workers [97] have found spatial separation of charge carrier by changing the size of the core and the shell in CdSe/ZnTe. Feldman and co-workers 16 reported charge separation and tunneling behavior between CdTe and CdSe QD material with the formation of core-shell structures. Banin and co-workers [98] focused on photophysical properties of ZnSe QD within CdS nanorods and demonstrate the charge separation. Most of the above studies have thrown light on the issue of charge separation clearly; however, still much more are to be understood for a device application. It is very important to be acquainted with how fast the electrons or holes are migrated to another semiconductor and also how fast the photoexcited carriers relaxed in different QD materials.

1.3 Photocatalysis phenomenon

A ‘‘photocatalytic reaction’’ can be defined as a chemical reaction induced by photoabsorption of a solid material, or ‘‘photocatalyst,’’ which remains unchanged during the reaction. Photocatalysis is often explained with the help of a schematic representation of the electronic structures of semiconducting materials, a band model; an electron in an electron-filled valence band (VB) is excited by photoirradiation to a vacant conduction band (CB), which is separated by a forbidden band, a band gap, from the VB, leaving a positive hole in the VB [99]. These electrons and positive holes take part in reduction and oxidation, respectively, of compounds adsorbed on the surface of a photocatalyst. This analysis explains the photocatalytic reactions of semiconducting and insulating materials absorbing photons by the bulk of materials. The Honda–Fujishima effect is a well-established chemical phenomenon closely related to photocatalysis [99]. Irradiation of a titania single-crystal electrode immersed

in an aqueous electrolyte solution under illumination generates oxygen evolution from the titania electrode and hydrogen evolution from a platinum counter electrode when some anodic bias is applied to the titania working electrode or chemical bias, e.g., making higher *pH* of an electrolyte solution for the working electrode, is given [99]. Photoexcited electrons and positive holes generated by photoabsorption are situated at close proximity to each other and interact with each other by electrostatic force. It has been already established that the photocatalyticreaction by titania and related photocatalysts under ultraviolet irradiation in the presence of air or oxygen decomposes organic compounds almost completely. Titania possessing higher photocatalytic activity compared with that of other metal oxides is due to its high reduction ability to inject photoexcited electrons into molecular oxygen adsorbed on the surface of photocatalysts [99].

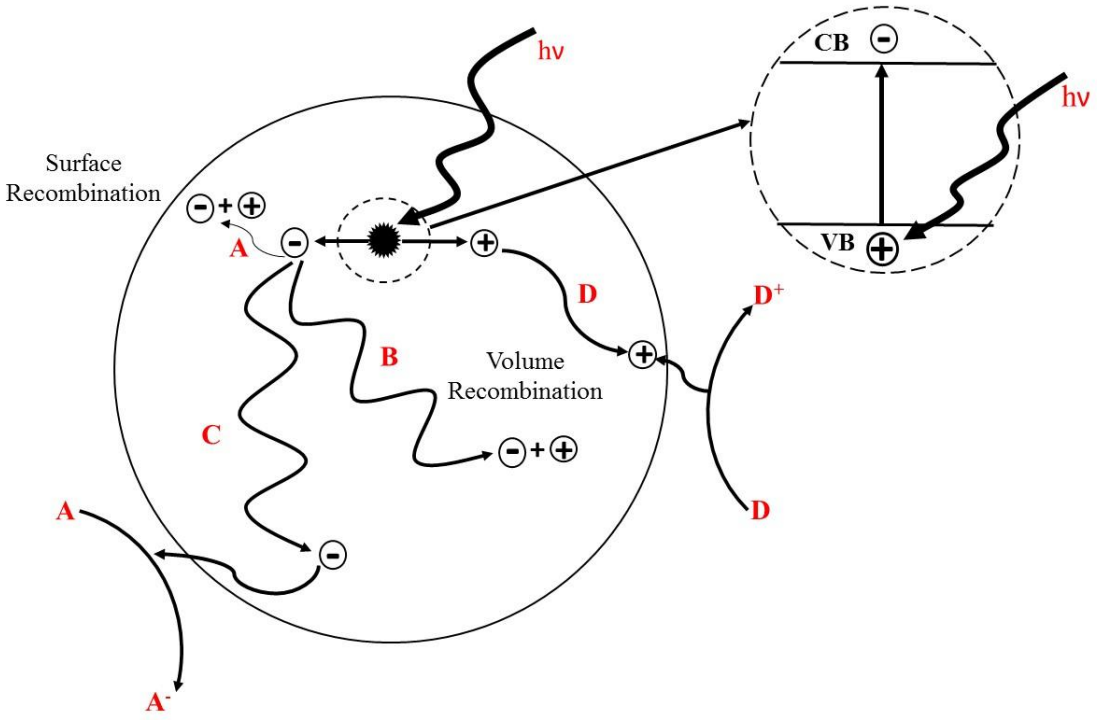

Fig 1.7: Schematic of mechanism of photocatalysis [148]

Functional one-dimensional metallic oxides have grabbed enormous interest because of their potential use in electronic, optical and spintronic devices [100-102]. Except titanium dioxide (TiO_2), zinc oxide (ZnO) and vanadium pentoxide (V_2O_5) nanostructures including nanowires, nanobelts and nanorods have been extensively

studied due to their special electronic, chemical and optical properties [103-104]. These metallic oxide materials are incorporated into an integrated structure with nanoscale dimension and the resulting hierarchical nanostructures often possess much large surface areas and improved physical and chemical properties, providing potential applications for sensing, light emission and photocatalysis [105-106]. Now a days , composite nanomaterials such as core-shell nanostructure are formed by the inside nanorods with the outside covered layers e.g TiO_2/ZnO, ZnO/MgO and ZnO/Er_2O_3 core-shell structures have been fabricated [107-110].

Currently much interest has been bestowed upon coupling different semiconductor particles with TiO_2, with coupled samples such as TiO_2-CdS, Bi_2S_3-TiO_2, TiO_2-WO_3, TiO_2-SnO_2, TiO_2-MoO_3, and TiO_2-Fe_2O_3being reported [111-114]. TiO_2 coated SnO_2 particles sizing 80-100 Å in diameter exhibited improved photochromic and photocatalytic efficiencies compared with TiO_2-capped SiO_2, TiO_2, SiO_2, and SnO_2 samples. Elder et al. [115] prepared TiO_2/MoO_3core-shell nanocrystalline material and found that photoabsorption energy of this system systematically shifted from 2.88 to 2.60 eV as the size of the composite nanoparticle was tuned from 80 to 40 Å. Still, these materials were found to exhibit a lower efficiency than Degussa P25 for the photocatalytic oxidation of acetaldehyde.

Again because of their size dependent absorption and emission properties CdSe nanoparticles have been the choices of many recent electron transfer investigations to study photocatalytic performances [116-120]

1.4 Photovoltaic (PV) effect

The photovoltaic effect is the creation of voltage or electric current in a material upon exposure to light.

The photovoltaic effect is directly related to the photoelectric effect, though they are different processes. When the sunlight or any other light is incident upon a material surface, the electrons present in the valence band can absorb energy and, being excited, jump to the conduction band and become free. These highly excited, non-thermal electrons diffuse, and some reach a junction where they are accelerated into a different material by a built-in potential (Galvani potential). This generates an

electromotive force, and thus some of the light energy is converted into electric energy. The photovoltaic effect can also occur when two photons are absorbed simultaneously in a process called two-photon photovoltaic effect [121]. When light is applied to the junction, one can model the solar cell as an ideal diode in parallel with a current source, J_L, that accounts for the photogenerated electron-hole pairs (excitons) in the semiconductor, and a resistive load. This can be combined with the standard diode equation to yield a general expression for a semiconducting p-n diode-based photovoltaic cell:

$$J = \ J_0 \left[\exp\left(\frac{qV}{\eta KT}\right) - 1\right] - J_L$$

where the photogenerated current density in a semiconductor of bandgap E_g is related to the applied light spectrum as

$$J_L = q \int_{h\nu=E_g}^{\infty} \frac{d\phi_{ph}}{dh\nu}\, d(h\nu)$$

Based on this expression, one can see that application of light to a PV device leads to a shift of the diode current-voltage (*I-V*) or current density/voltage (J-V) equation into the fourth quadrant (fig 1.8), and thus also leads to power generation that can be applied to a load (the area under the curve) [122].The *J-V* plot contains several critical parameters that directly relate to the efficiency of the solar cell. The short-circuit current density (or current), J_{sc}, provides the maximum current density that is obtainable when the two leads of the device are connected, i.e., under no load. The maximum J_{sc} available from the AM1.5 solar spectrum to a single-bandgap solar cell (which is directly related to the integrated solar photon flux)

V_{oc} derived from the ideal diode law:

$$V_{oc} \ = \frac{KT}{q}\ln\left(\frac{I_L}{I_o} + 1\right) \approx \frac{KT}{q}\ln(\frac{I_L}{I_O})$$

Another important feature of the *J-V* curve is the so-called fill factor (FF). This quantifies the "squareness" of the *J-V* curve under solar illumination, and can be

defined as the ratio of the area of the curve under the maximum power point of the cell (fig 1.8), i.e., $P_{max}= I_{max}V_{max}$, to the area associated with open and closed circuit ($P = I_{sc}V_{oc}$) [122]. These parameters directly relate to the power conversion efficiency of the device, η, under direct sunlight as

$$\eta = \frac{I_m V_m}{P_O} = A\, J_{sc}\, V_{oc}\, FF/P_O$$

which Po is the applied power density to the device.

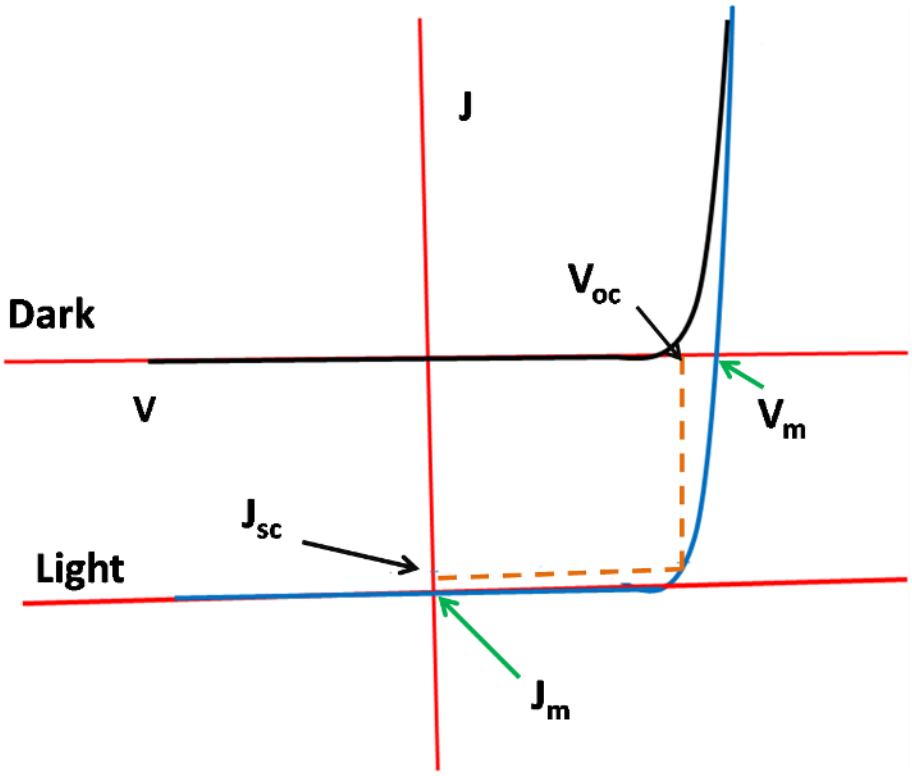

Fig. 1.8 *J-V* curve of a photovoltaic cell [122]

The juncture of photovoltaics and nanotechnology, i.e., nanophotovoltaics (nano-PV) is a relatively recent trend. While some nanostructure-related concepts were studied in the 1980s and early 1990s, particularly as related to nanocrystalline silicon thin films, it is only in this decade that the use of various emerging classes of nanostructures has been applied to PV. An early example of using nanostructured materials was shown by Grätzel and coworkers, who used compacted and annealed nano-sized titania powders to demonstrate a dye-sensitized solar cell [131]. Perhaps one of the first attempts at

utilizing distinct emerging nanostructures in PV was 2010 by Taylor and Francis Group, LLC by Alivisatos and coworkers, who used CdSe nanocrystals in combination with organic hole conducting layers to make a novel solar cell with a power conversion efficiency of 1.7% [122].

Among the inorganic materials proposed as a PV alternative to silicon, cuprous oxide (Cu_2 O) is one of the most extensively studied, with investigations stretching back more than 20 years. As-made Cu_2O is a p-type semiconductor with a band gap of 2.0 eV, which allows for good solar spectral absorption [123]. The abundance and non toxicity of copper, as well as the long-term stability associated with oxides, allows for the possibility of constructing durable, long-lasting solar cells with Cu2Oasthe active light-absorbing component. There are several examples of Cu_2O-based PV devices reported in the literature, often prepared by using low-cost, solution-based methods [124-125]. Nanowire-based solar cells have been reported to possess inherent advantages over traditional bilayer devices [128-129] In addition, oriented nanowire arrays have been shown to possess excellent charge transport (and therefore charge collection) characteristics in photovoltaic devices [126-127]. Our solar cell consists of vertically oriented n-type zinc oxide nanowires, surrounded by a film constructed from p-type cuprous oxide nanoparticles. Our solution-based synthesis of inexpensive and environmentally benign oxide materials in a solar cell would allow for the facile production of large-scale photovoltaic devices. We found that the solar cell performance is enhanced with the addition of an intermediate oxide insulating layer between the nanowires and the nanoparticles.

Dye-sensitized solar cells based on nanocrystalline TiO_2 photoelectrode are of great interest as an alternative to the conventional silicon solar cells because of their high performance and low-cost production [130-132]. In application to DSCs, vertically oriented TiO_2 nanotube arrays have higher charge collection efficiencies than a nanoparticle-based structure due to their faster transport and slower recombination of electrons [133-134]. On the other hand, coating surface of the nanocrystalline photoelectrode with a high energy band-gap material has received much attention for enhancing the photovoltaic performance [135-136]. These coating layers retard back transfer of electrons to the electrolyte thereby minimizing charge recombination [135-139]. Moreover, dye attachment becomes more favorable because the surface of

coating material is more basic than TiO_2, and consequently, a light harvesting efficiency can be increased [135-137].

C.O.Avelleneda and his co-workers studied DSSC based on TiO_2 electrodes coated with various thin oxide layers such as Al_2O_3, Nb_2O_5, MgO and $SrTiO_3$. No significant changes were observed for the short-circuit current density due to the different coating layers, but The Voc values changed notably: from 0.73 V (for TiO_2electrodes) to 0.78 V for TiO_2-MgO core-shell electrodes[140]. The latter electrodes provided DSSC endowed with overall energy conversion efficiencies as high as 5% under 1 sun.

Thus, it became a well known fact that , a common technique to control and enhance the properties of nanostructures is to create core–shell heterostructures [141-148] The addition of a shell often modifies the electronic nature of the original material, by enhancing the interaction with the surrounding medium without altering the properties, both optical and electrical, of the core structure. Low temperature synthesis of nanostructures, such as quantum dots [143-144], and nanowires [145-146], are a key area of importance, with device applications in various fields [142-144, 146]. A novel low temperature hydrothermal synthesis of ZnO– MgO core–shell NWs was found to be a successful and inexpensive method of producing uniform, functional nanostructures [141]. The hydrothermally grown MgO layers enhanced the photocurrent and open-circuit voltage of solid state dye-sensitized solar cells, producing a five-fold increase in power conversion efficiency, as measured under AM1.5 simulated sun light.

1.5 Motivation of our work

As we have already explained in the previous sections, core-shell nanomaterials have caught enormous interest as useful material for photocatalysis or photovoltaic purpose. For a device application a material must possess three criterions [147] In organic or polymeric solar cells, device operation involves (1) exciton generation, (2) charge separation, and (3) carrier transport to the opposite electrodes [147] Since the three steps occur in sequence, efforts have been made to enhance efficiency or output of each of the steps. Generation of excitons expectedly depends on matching of electronic absorption spectrum of the active material with that of the solar illumination. Hence

active materials are chosen accordingly. Exciton dissociation or charge separation, which occurs at the interface between a donor and an acceptor layer, takes place due to the internal field that develops owing to the difference of energy levels at the interfaces. Carrier transport, the third step, is directed by the internal field generated by the difference in work functions of the two electrodes. Also the interesting properties exhibited by core-shell nanostructures which are quite different than the core or shell itself was a major reason to carry out our research work on these functional nanomaterials.

We have also described in section that environmental clean up has been an important issue now a days due to increasing amount of waste water from industries which are adverse effects of improving civilization. TiO_2 is already been established as a good photocatalyst for decomposition of waste water of dyes which are very toxic. Our effort was to observe what influence on the photocatalytic properties can be seen if we coat the material TiO_2 with some other oxide materials of different band gaps (MgO= 7.8 eV, SnO_2= 3.7 eV and ZrO_2 = 5.7 eV). Out of these materials TiO_2/MgO and TiO_2/SnO_2 has been studied extensively in earlier reports also. But our aim was to make a comparative study of photocatalytic activity of these materials to know which coating was best to get better result. Also we synthesized a novel core-shell material Ag_2S-HgS whose photocatalytic efficiency is compared with TiO_2 based materials.

We have studied photovoltaic performance of TiO_2 and other related core-shell nanostructures via a very simple cost effective laboratory method. These electrodes are sensitized with dye (EOSINY) to extend the absorbance regime to visible region so that we can attain practical application. The fill factors we obtained were quite satisfactory and one can expect that highly efficient photovoltaic devices can be fabricated from these core-shell nanostructures with better and sophisticated equipments.

References

[1] The Nanotechnology R(evolution)1 Charles Tahan Cavendish Laboratory, University of Cambridge, JJ Thomson Ave, Cambridge, CB3 0HE, UK.

[2] Chapter 1 - 2011 nanomaterial, A. Alagarasi, pp 76,india

[3] Blackman. J (ed.), *Metallic nanopartcles*, Elsevier, Oxford, 2009 [4] Bonnemann.H., & Richards, R.M. Nanoscopic Metal Particles − Synthetic Methods and Potential Applications, *Eur.J.Inorg.Chem.***2001**(10) 2455--2480, 2001.

[5] K.E.Drexler, Engines of Creation, Knopf Doubleday Publishing Group (1987).

[6] Roduner, E., Size matters: why nanomaterials are different, *Chem. Soc. Rev*. **35**, 583--592, 2006.

[7] Lu,Y.,et al. Modifying the Surface Properties of Superparamagnetic Iron Oxide Nanoparticles through A Sol−Gel Approach, *Nanoletters* **2**,183--186, 2002.

[8] J.H.Davis, Physics of Low dimensional Structures, Cambridge (1998)

[9] Liz-Marzan, L.M., Nanometals: Formation and color, *Mater.Today*, **7**(2) , 26--31,2004.

[10] Nanda, K.K., et al. Energy Levels in Embedded Semiconductor Nanoparticles and Nanowires, *Nano Letters***1**,605—611,2011.

[11] Zhang,S., et al. Relative Influence of Surface States and Bulk Impurities on the Electrical Properties of Ge Nanowires, *Nano Lett*.**9**,3268--3274 , 2009.

[12] Jiang,M.Y., et al. Role of surface electronic transitions in linear and nonlinear electromagnetic phenomena at noble metal surfaces: beyond jellium, *Surface Science* **242**,306--313,1991.

[13] Chen,X., & Mao, S. S., Titanium Dioxide Nanomaterials: Synthesis, Properties, Modifications, and Applications, *Chem.Rev*. **107**,2891--2959, 2007.

[14] Yoffe, A.D., Low-dimensional systems: quantum size effects and electronic properties of semiconductor microcrystallites (zero-dimensional systems) and some quasi-two-dimensional systems, *Advances in Physics* **42** (993) 173--262.

[15] Wang, Y., & Herron, N. Nanometer-sized semiconductor clusters: materials synthesis, quantum size effects, and photophysical properties, *J.Phys.Chem* **95** , 525--532, 1991.

[16] Fundamentals of nanomaterials https://www.ttu.ee/public/m/mehaanikateaduskond/Instituudid/Materjalitehnika_instituut/MTX9100/Lecture5_NanomatFundamentals.pdf

[17] Tang, D.Y, et al. Observation of High-Order Polarization-Locked Vector Solitons in a Fiber Laser, *Phy.Rev.Lett*.**101**,153904 (1--4),2008.

[18]http://homes.nano.aau.dk/kp/Quantum%20size%20effects%20in%20nanostructures.pdf

[19] Chaudhuri, R.G., & Paria,S., Core/Shell Nanoparticles: Classes, Properties, Synthesis Mechanisms, Characterization, and Applications, *Chem. Rev*.**112**, 2373--2433, 2012.

[20] Oldenburg, S. J., et al. Nanoengineering of optical resonances, *Chemical Physics Letters* **288** (2–4), 243--247, 1998.

[21] Daniel, M. C., & Astruc, D. Gold Nanoparticles: Assembly, Supramolecular Chemistry, Quantum-Size-Related Properties, and Applications toward Biology, Catalysis, and Nanotechnology, *Chem. Rev.***104** (1), 293--346, 2004.

[22] Caruso, F., Nanoengineering of Particle Surfaces , *Adv. Mater.***13**, 11--12,2001.

[24] Kalele, S., et al. Nanoshell Particles: synthesis, properties and applications, *Current Science* **91**(8), 1038--1052, 2006.

[25] Balakrishnan, S., et al Particle size effect on phase and magnetic properties of polymer-coated magnetic nanoparticles , *Journal of Magnetism and Magnetic Materials* **321** (2) ,117--122,2009.

[26] Salgueiriño-Maceira, V., & Correa-Duarte , M.A., Increasing the Complexity of Magnetic Core/Shell Structured Nanocomposites for Biological Applications, *Adv. Mater.* **19**, 4131--4144, 2007.

[27] Phadtare, S., et al. Direct Assembly of Gold Nanoparticle "Shells" on Polyurethane Microsphere "Cores" and Their Application as Enzyme Immobilization Templates, *Chem. Mater.***15** (10), 1944--1949, 2003.

[28] Kortan, A. R., et al. Nucleation and growth of cadmium selendie on zinc sulfide quantum crystallite seeds, and vice versa, in inverse micelle media, *J. Am. Chem. Soc.* 112 (4),1327--1332, 1990.

[29] Qi, L., et al. Synthesis and characterization of mixed CdS-ZnS nanoparticles in reverse micelles, *Colloids and Surfaces A: Physicochemical and Engineering Aspects,*111(3) , 195--202, 1996.

[30] Mews, A., et al. Preparation, characterization, and photophysics of the quantum dot quantum well system cadmium sulfide/mercury sulfide/cadmium sulfide, *J.Phys.Chem*, 98,934--941,1994.

[31] Kamat,P.V., & Shanghavi,B. Interparticle Electron Transfer in Metal/Semiconductor Composites. Picosecond Dynamics of CdS-Capped Gold Nanoclusters, *J. Phys. Chem. B,* 101 (39), 7675--7679, 1997.

[32] Scodeller, P., et al. Wired-Enzyme Core−Shell Au Nanoparticle Biosensor,

*J. Am. Chem. Soc.***130**, 12690--12697,2008.

[33] Laurent, S., et al.Magnetic Iron Oxide Nanoparticles: Synthesis, Stabilization, Vectorization, Physicochemical Characterizations, and Biological Applications **,***Chem. Rev.* **108**, 2064--2110,2008.

[34] Babes,L., et al. Synthesis of Iron Oxide Nanoparticles Used as MRI Contrast Agents: A Parametric Study, *Journal of Colloid and Interface Science* **212**(2), 474--482, 1999

[35] Dresco,P.A., et al. Preparation and Properties of Magnetite and Polymer Magnetite Nanoparticles, *Langmuir*, 15 (6), 1945--1951, 1999

[36] Sounderya, N., & Zhang, Y. Use of core/shell structured nanoparticles for biomedical applications, *Recent Patents on Biomedical Engineering* **1** (1), 34--42, 2010.

[37] Gupta, A.K., & Gupta,M. Synthesis and surface engineering of iron oxide nanoparticles for biomedical applications, *Biomaterials* **26**(18), 3995--4021, 2005.

[38] Yan, E et. al. Polymer/silica hybrid hollow nanospheres with pH-sensitive drug release in physiological and intracellular environments, *Chem. Commun.*19, 2718--2720, 2009.

[39] Jaiswal,J.K et al. Long-term multiple color imaging of live cells using quantum dot bioconjugates *Nature Biotechnology* **21**, 47--51,2003

[40] Michalet , X., et al. Quantum Dots for Live Cells, in Vivo Imaging, and Diagnostics *Science* **307,** 538--544,2005

[41] De, M., et al Applications of Nanoparticles in Biology , *Adv. Mater*. **20**, 4225--4241) , 2008.

[42] Correa-Duarte, M. A., et al. Stabilization of CdS semiconductor nanoparticles against photodegradation by a silica coating procedure, *Chemical Physics Letters* 286 (5–6)17, 497--501, 1998.

[43] Gerion, D., et al. Synthesis and Properties of Biocompatible Water-Soluble Silica-Coated CdSe/ZnS Semiconductor Quantum Dots, *J. Phys. Chem. B*, 105 (37), 8861--8871, 2001.

[44] Talapin, D. V., et al. CdSe/CdS/ZnS and CdSe/ZnSe/ZnS Core−Shell−Shell Nanocrystals, *J. Phys. Chem. B.* **108** (49), 18826--18831, 2004.

[45] Lambert, K., et al. PbTe|CdTe Core|Shell Particles by Cation Exchange, a HR-TEM study *Chem. Mater*. **21** (5), 778--780, 2009.

[46] Dorfs, D., et al. Type-I and Type-II Nanoscale Heterostructures Based on CdTe Nanocrystals: A Comparative Study , *Small* **4**, 1148--1152, 2008.

[47] Ivanov, S. A., et al. Type-II Core/Shell CdS/ZnSe Nanocrystals: Synthesis,Electronic Structures, and Spectroscopic Properties, *J. Am. Chem. Soc.* **129**, 11708--11719, 2007.

[48] Tian, Y., et al. Coupled Composite CdS−CdSe and Core−Shell Types of (CdS)CdSe and (CdSe)CdS Nanoparticles, *J. Phys. Chem.***100**, 8927--8939, 1996.

[49] Xie, W., et al. STRUCTURE AND SPECTRAL CHARACTERISTICS OF CdS/CdSe, *J. Chin Ceram. Soc.***37**, 219--224,2009.

[50] Kim, S.; et al. Type-II Quantum Dots: CdTe/CdSe(Core/Shell) and CdSe/ZnTe(Core/Shell) Heterostructures , *J. Am. Chem. Soc.***125** (38),11466--11467, 2003.

[51] Oron, D., et al. Multiexcitons in type-II colloidal semiconductor quantum dots, *Phys. Rev. B.* **75**, 035330(1--7), 2007.

[52] Scheops, O., et al. Recombination Dynamics of CdTe/CdS Core−Shell Nanocrystals, *J. Phys. Chem. B* **110**, 2074--2079 , 2006.

[53] Xie,R.,et al. Synthesis, Characterization, and Spectroscopy of Type-II Core/Shell Semiconductor Nanocrystals with ZnTe Cores , *Adv. Mater.* 17, 2741--2745, 2005.

[54] Bang,J., et al.ZnTe/ZnSe (Core/Shell) Type-II Quantum Dots: Their Optical and Photovoltaic Properties *Chem. Mater.* **22** (1), 233--240, 2010.

[55] Pietryga, J. M., et al. Utilizing the Lability of Lead Selenide to Produce Heterostructured Nanocrystals with Bright, Stable Infrared Emission, *J. Am. Chem. Soc.***130** (14),4879--4885, 2008.

[56] Ivanov, S. A., et al. Light Amplification Using Inverted Core/Shell Nanocrystals: Towards Lasing in the Single-Exciton Regime, *J. Phys. Chem. B.* **108** (30),10625--10630, 2004.

[57] Subramanian, R., et al. A novel technique for synthesis of silver nanoparticles by laser-liquid interaction, *J.Mater.Sci.* **33**, 3471--3477, 1998.

[58] Jang, D.; Oh, B.; Kim, D. Proc. SPIE2002, 1024.

[59] Hong, L. I., et al**.** Laser beam processing of a SiC particulate reinforced aluminium metal matrix composite **,** *J. Mater. Sci.* **32**, 5545--5550, 1997.

[60] Dodd,A.C., A comparison of mechanochemical methods for the synthesis of nanoparticulate nickel oxide , *Powder Technology* **196** (1), 30--35, 2009**.**

[61] Sasikumar, R., & Arunachalam, R.M. Synthesis of nanostructured aluminium matrix composite (AMC) through machining, *Materials Letters* **63** , 2426--2428 , 2009.

[62] Kim, H., et al. Synthesis and Characterization of Co/CdSe Core/Shell Nanocomposites: Bifunctional Magnetic-Optical Nanocrystals, *J. Am. Chem. Soc.* **127**, 544--546, 2005.

[63] Caruso, R. A., et al. Multilayered Titania, Silica, and Laponite Nanoparticle Coatings on Polystyrene Colloidal Templates and Resulting Inorganic Hollow Spheres, *Chem. Mater.***13**, 400--409, 2001.

[64] Oyama, H.T.et al. Coating of Uniform Inorganic Particles with Polymers, *Journal of Colloid and Interface Science* **160** (2), 298--303, 1993.

[65] Wang, L., Monodispersed Core−Shell Fe_3O_4@Au Nanoparticles, *J. Phys. Chem. B.* **109**, 21593--21601, 2005.

[66] Kobayashi, Y., et al. Preparation and Properties of Silica-Coated Cobalt Nanoparticles , *J. Phys. Chem. B.* **107**, 7420 --7425, 2003.

[67] Imhof, A., Preparation and Characterization of Titania-Coated Polystyrene Spheres and Hollow Titania Shells , *Langmuir***17**, 3579--3585,2001.

[68] Ocana, M., et al. Preparation and properties of uniform-coated colloidal particles : Titania on zinc oxide, *Langmuir* **7**, 2911--2916, 1991.

[69] Zou, H.; et al. Polymer/Silica Nanocomposites: Preparation, Characterization, Properties, and Applications, *Chem. Rev.* **108**, 3393--3957, 2008.

[70] Okaniwa, M. J., Synthesis of poly(tetrafluoroethylene)/poly(butadiene) core-shell particles and their graft copolymerization, *Appl. Polym. Sci.* **68**, 185--190, 1998.

[71] Shenoy, D. B., et al. Layer-by-Layer Engineering of Biocompatible,Decomposable Core−Shell Structures, *Biomacromolecules* **4**, 265--272, 2003.

[72] Srivastava, S., & Kotov, N. A. Composite Layer-by-Layer (LBL) Assembly with Inorganic Nanoparticles and Nanowires, *Acc. Chem. Res.* **41**, 1831--1841, 2008.

[73] Wu, T. M., & Chu, M. S . Preparation and characterization of thermoplastic vulcanizate/silica nanocomposites , *J. Appl. Polym. Sci.* **98**, 2058 --2063, 2005

[74] Hofman-Caris, C. H. M. *New J. Chem.***18**, 1087--1096, 1994.

[75] Das, K., & De, S.K., Optical Properties of the Type-II Core-Shell TiO2@CdS Nanorods for Photovoltaic Applications, *J. Phys. Chem. C.***113**, 3494--3501,2009.

[76] Gerischer, H., & Lübke, M. A particle size effect in the sensitization of TiO_2 electrodes by a CdS deposit, *Journal of Electroanalytical Chemistry and Interfacial Electrochemistry***204**(1–2), 225--227, 1986.

[77] Vogel, R., et al. Quantum-Sized PbS, CdS, Ag2S, Sb2S3, and Bi2S3 Particles as Sensitizers for Various Nanoporous Wide-Bandgap Semiconductors, *J. Phys. Chem.* **98**, 3183--3188, 1994.

[78] Plass, R., Quantum Dot Sensitization of Organic−Inorganic Hybrid Solar Cells, *J. Phys. Chem. B.* **106**, 7578--7580, 2002.

[79] Robel, I., et al. Size-Dependent Electron Injection from Excited CdSe Quantum Dots into TiO_2 Nanoparticles, *J. Am. Chem. Soc.***129**,4136--4137, 2007.

[80] Zaban, A., et al. Photosensitization of Nanoporous TiO_2 Electrodes with InP Quantum Dots, *Langmuir***14**, 3153--3156, 1998.

[81] Shenyuan , Y., et al. Strain-Induced Band Gap Modification in Coherent Core/Shell Nanostructures , *Nano Lett.***10**, 3156--3162, 2010.

[82] Dabbousi, B. O., et al. (CdSe)ZnS Core−Shell Quantum Dots: Synthesis and Characterization of a Size Series of Highly Luminescent Nanocrystallites, *J. Phys. Chem. B.* **101**(46), 9463--9475, 1997.

[83] Chin, P. T. K., et al. Highly Luminescent CdTe/CdSe Colloidal Heteronanocrystals with Temperature-Dependent Emission Color, *J. Am. Chem. Soc.***129**(48), 14880--14886, 2007.

[84] Peng, X., et al. Epitaxial Growth of Highly Luminescent CdSe/CdS Core/Shell Nanocrystals with Photostability and Electronic Accessibility, *J. Am. Chem. Soc.* **119**(30), 7019--7029, 1997.

[85] Raychaudhuri, S., & Yu, E. T. Calculation of critical dimensions for wurtzite and cubic zinc blende coaxial nanowire heterostructures, *J. Vac. Sci. Technol. B.* **24**(4), 2053--2059, 2006.

[86] Smith, D. L.; Mailhiot, C. Theory of semiconductor superlattice electronic structure, *Rev. Mod. Phys.***62**(1), 173--234, 1990.

[87] Owen, J. S., et al. Reaction Chemistry and Ligand Exchange at Cadmium−Selenide Nanocrystal Surfaces, *J. Am. Chem. Soc.***130**(37), 12279--12281,2008.

[88] Schops, O., et al. Recombination Dynamics of CdTe/CdS Core−Shell Nanocrystals,*J. Phys. Chem. B.* **110**, 2074--2079, 2006.

[89] Yu, K., et al. Sequential Synthesis of Type II Colloidal CdTe/CdSe Core–Shell Nanocrystals, *Small* **1,** 332--338, 2005.

[90] Xie, R., et al. Synthesis, Characterization, and Spectroscopy of Type-II Core/Shell Semiconductor Nanocrystals with ZnTe Cores, Adv. Mater.**17**, 2741--2745,2005.

[91] Balet, L. P., et al. Inverted Core/Shell Nanocrystals Continuously Tunable between Type-I and Type-II Localization Regimes, *Nano Lett.* **4**, 1485--1488, 2004.

[92] Kaniyankandy, S., et al. Ultrafast Hole Transfer in CdSe/ZnTe Type II Core-Shell Nanostructure, *J. Phys. Chem. C.***115**, 1428--1435, 2011.

[93] Burda, C., et al. Electron Shuttling Across the Interface of CdSe Nanoparticles Monitored by Femtosecond Laser Spectroscopy, *J. Phys.Chem. B.* **103**, 1783--1788, 1999.

[94] Boulesbaa, A., et al. Ultrafast Charge Separation at CdS Quantum Dot/Rhodamine B Molecule Interface, *J. Am. Chem. Soc.*129, 15132--15133,2007.

[95] Dooley, C. J., et al. Ultrafast Electron Transfer Dynamics in CdSe/CdTe Donor−Acceptor Nanorods, *J. Phys. Chem. C.*112, 12074--12076, 2008.

[96] Garca-Santamara, F., et al. Suppressed Auger Recombination in "Giant" Nanocrystals Boosts Optical Gain Performance, *Nano Lett.***9**, 3482--3488, 2009.

[97] Chen, C. Y., et al. Spectroscopy and Femtosecond Dynamics of Type-II CdSe/ZnTe Core−Shell Semiconductor Synthesized via the CdO Precursor, *J. Phys. Chem. B.***108**, 10687--10691, 2004.

[98] Dorfs, D., et al. ZnSe Quantum Dots Within CdS Nanorods: A Seeded-Growth Type-II System, *Small***4**, 1319--1323, 2008.

[99] Bunsho, O., Preparing Articles on Photocatalysis—Beyond the Illusions, Misconceptions, and Speculation, *Chemistry Letters* **37** (3), 216--229, 2008.

[100] Zou, C.W., & Gao, W. Fabrication, Optoelectronic and Photocatalytic Properties of Some Composite Oxide Nanostructures, *Trans. Electr. Electron. Mater*. **11**(1) 1--10, 2010.

[101] Kong, X.Y., & Wang, Z.L. Spontaneous Polarization-Induced Nanohelixes, Nanosprings, and Nanorings of Piezoelectric Nanobelts, *Nano Lett.***3**, 1625--1631,2003.

[102] Bao, J., et al. Broadband ZnO Single-Nanowire Light-Emitting Diode, *Nano Lett.* **6**, 1719--1722,2006.

[103] Kim,Y.K., et al. Control of adsorption and alignment of V_2O_5 nanowires via chemically functionalized patterns, *Nanotechnology* **18**, 015304(1--6), 2007.

[104] Wang, R., et al. TiO_2 Nanowire Bundle Microelectrode Based Impedance Immunosensor for Rapid and Sensitive Detection of Listeria monocytogenes, *Nano Lett.* 8, 2625--2631,2008.

[105] Gao, W., & Li, Z., Nanostructures of zinc oxide, *Int. J. Nanotechnol.* **6**, 245--257, 2009.

[106]Rackauskas,S.,et al. A novel method for metal oxide nanowire synthesis,*Nanotechnology* **20**, 165603(1--8), 2009.

[107] Greene,L.E., et al. ZnO−TiO_2 Core−Shell Nanorod/P3HT Solar Cells, *J. Phys. Chem. C*. **111**, 18451--18456,2007.

[108] Mustafa, D.,et al.Structural characterization of ZnO/ Er_2O_3 core/shell nanowires, *Superlattices Microstruct.* **42**, 403--408,2007.

[109] Li, S.Z., et al. Enhanced photoluminescence of ZnO/Er2O3 core-shell structure nanorods synthesized by pulsed laser deposition, *Appl. Phys. Lett.* **90**, 263106,2007.

[110]Kaydashev,V. E., et al.Structural and optical properties of Zn0.9Mn0.1O/ZnO core-shell nanowires designed by pulsed laser deposition,*J. Appl. Phys.* **106**, 093501,2009.

[111] Gupta S. M., & Tripathi, M. A review of TiO2nanoparticles, *Chinese Sci Bull.* **56 (**16), 1639--1657,2011.

[112] Vogel,R., et al. Quantum-sized PbS, CdS, Ag2S, Sb2S3, and Bi2S3particles as sensitizers for various nanoporous wide- bandgap semiconductors. *J.Phys.Chem.***98**, 3183--3188, 1994.

[113] Nayak, B.B., et al. Structural characterization of Bi2−xSbxS3films prepared by the dip-dry method. *Thin Solid Film*,**105**,17--24, 1983.

[114] Grandcolas,M., et al. Porogen template assisted TiO2rutile coupled nanomaterials for improved visible and solar light photocatalytic applications, *Catal Lett*,**123**,65--71, 2008.

[115] Elder,S. H., et al. The discovery and study of nanocrystalline TiO2-(MoO3) core-shell materials, *J. Am. Chem. Soc*.**122**,5138--6146, 2000.

[116] Harris,C., & Kamat,P.V. Photocatalysis with CdSe Nanoparticles in Confined Media: Mapping Charge Transfer Events in the Subpicosecond to Second Timescales, *ACS NANO* **3**(3), 682--690, 2009.

[117] Dimitrijevic, N. M. Electron-Transfer Reactions on CdSe Colloids as Studied by Pulse Radiolysis. *J. Chem. Soc., Faraday Trans. 1*.**83**, 1193--1201,1987.

[118] Robel, I.; et al. Quantum Dot Solar Cells. Harvesting Light Energy with CdSe Nanocrystals Molecularly Linked to Mesoscopic TiO2 Films, *J. Am. Chem. Soc*.**128,** 2385--2393, 2006.

[119] Ginger, D. S.; & Greenham, N. C. Photoinduced ElectronTransfer from Conjugated Polymers to CdSe Nanocrystals, *Phys. Rev. B* **59**, 10622--10629,1999.

[120] Jones, M.; et al. Exciton Trapping and Recombination in Type II CdSe/CdTe Nanorod Heterostructures, *J. Phys. Chem. C*. **112**, 5423--5431, 2008.

[121] http://en.wikipedia.org/wiki/Photovoltaic_effect

[122] Tsakalakos, L. (ed.) *Nanotechnology for photovoltaic* CRC Press Taylor & Francis Group, New York, 2010.

[123] Yuhas, B. D., & Yang,P. Nanowire-Based All-Oxide Solar Cells, *J. Am. Chem. Soc.* **131**, 3756--3761, 2009.

[124] Minami, T., et al. Effect of ZnO film deposition methods on the photovoltaic properties of ZnO–Cu_2O heterojunction devices,*Thin Solid Films* **494**,47--52,2006.

[125] Akimoto, K., et al. Thin film deposition of Cu_2O and application for solar cells ,*Solar Energy* **80**, 715--722, 2006.

[126] Adachi,M.,et al. Dye-Sensitized Solar Cells Based on Anatase TiO_2Nanoparticle/Nanowire Composites, *J. Phys. Chem.B.***110**,15932--15938, 2006 .

[127] Meng, S., et al. Natural Dyes Adsorbed on TiO_2 Nanowire for Photovoltaic Applications: Enhanced Light Absorption and Ultrafast Electron Injection, *Nano Lett.***8**, 3266--3272,2008.

[128] Garnett, E. C.; & Yang, P. Silicon Nanowire Radial p−n Junction Solar Cells, *J. Am. Chem. Soc.* **130**, 9224--9225, 2008.

[129] Tian, B., et al. Coaxial silicon nanowires as solar cells and nanoelectronic power sources, *Nature* **449**, 885--889, 2007.

[130] Park, H., et al. Fabrication of MgO-coated TiO2nanotubes and application to dye-sensitized solar cells, *J.Electroceram.***23**, 146--149, 2009.

[131] O'Regan, B., & Gratzel, M. , A low-cost, high-efficiency solar cell based on dye-sensitized colloidal TiO2 films, *Nature* **353**, 737--740,1991.

[132] Barbe, C. J., et al. Nanocrystalline Titanium Oxide Electrodes for Photovoltaic Applications, *J. Am. Ceram. Soc.***80**, 3157--3171,1997.

[133] Zhu, K., et al. Enhanced Charge-Collection Efficiencies and Light Scattering in Dye-Sensitized Solar Cells Using Oriented TiO_2 Nanotubes Arrays, *Nano Lett.***7**(1), 69--74, 2007.

[134] Shankar, K., et al. Highly-ordered TiO2 nanotube arrays up to 220 μm in length: use in water photoelectrolysis and dye-sensitized solar cells *Nanotechnology***18**, 065707(1--11), 2007.

[135] Kay, A., & Gratzel, M. Dye-Sensitized Core−Shell Nanocrystals: Improved Efficiency of Mesoporous Tin Oxide Electrodes Coated with a Thin Layer of an Insulating Oxide, *Chem. Mater.***14**, 2930--2935 ,2002.

[136] Jung, H.S., et al. Preparation of Nanoporous MgO-Coated TiO_2 Nanoparticles and Their Application to the Electrode of Dye-Sensitized Solar Cells, *Langmuir***21**, 10332--10335,2005.

[137] Wang, Z.S., et al. Electronic-Insulating Coating of $CaCO_3$ on TiO_2 Electrode in Dye-Sensitized Solar Cells: Improvement of Electron Lifetime and Efficiency, *Chem. Mater.***18**, 2912--2916,2006.

[138] Fabregat-Santiago, F., et al. The origin of slow electron recombination processes in dye-sensitized solar cells with alumina barrier coatings, *J. Appl. Phys.***96**(11), 6903,2004.

[139] Chen, S. G., et al. Preparation of Nb_2O_5 Coated TiO_2 Nanoporous Electrodes and Their Application in Dye-Sensitized Solar Cells, *Chem. Mater*.**13**,4629--4634,2001.

[140] Avellaneda,C.O., et al. Preparation and characterization of core-shell electrodes for application in gel electrolyte-based dye-sensitized solar cells, *Electrochimica Acta* **55**,1468--1474, 2010.

[141] Plank, N.O.V., et al. A simple low temperature synthesis route for ZnO–MgO core–shell nanowires, *Nanotechnology***19**, 465603(1--8), 2008.

[142] Hodes,G.,When small is different: some recent advances in concepts and applications of nanoscale phenomena, *Adv. Mater.***19**, 639--655, 2007.

[143] Alivisatos ,A .P., Semiconductor clusters, nanocrystals, and quantum dots, *Science***27,**1933--1937, 1996.

[144] Mews, A., et al. Preparation, characterization, and photophysics of the quantum dot quantum well system cadmium sulfide/mercury sulfide/cadmium sulfide, *J. Phys. Chem.***98,**934–41, 1994.

[145] Rao, C.N.R., et al. Synthesis of inorganic nanomaterials, *Dalton Trans*.343728, 2007.

[146] Heo,Y,W., et al. ZnO nanowire growth and devices, *Mater.Sci. Eng.R.***47**,1--47, 2004.

[147] Kim,S., et al. Growth and enhanced light emission of hybrid structures of ZnO/Si nanocrystals, *Appl. Phys. Lett*. **922**, 43108--3, 2008.

[148] Lee,S.S.,et al. Homogeneous ZnS coating onto TiO2 nanoparticles by a simple one pot sonochemical method , *Chem. Eng. J.* **139**, 194--7,2008.

[147] Guchhait, A., et al. Hybrid Core-Shell Nanoparticles: Photoinduced Electron-Transfer for Charge Separation and Solar Cell Applications, *Chem. Mater*.**21**,5292--5299, 2009.

[148] Linsebigler, A.L., et al. Photocatalysis on TiO2 Surfaces: Principles, Mechanisms, and Selected Results, *Chem. Rev.* **95**, 735--758, 1995.